Arbitrary Trajectory Foot Planner for Bipedal Walking

Ramil Khusainov[1], Artur Sagitov[2], Alexandr Klimchik[1] and Evgeni Magid[2]

[1]*Intelligent Robotic Systems Laboratory, Innopolis University, Innopolis City, Russian Federation*
[2]*Higher Institute of Information Technology & Information Systems, Kazan Federal University, Kazan, Russian Federation*

Abstract: This paper presents a foot planner algorithm for bipedal walking along an arbitrary curve. It takes a parametrically defined desired path as an input and calculates feet positions and orientations at each step. Number of steps that are required to complete the path depends on a maximum step length and maximum foot rotation angle at each step. Provided with results of the foot planner, our walking engine successfully performs robot locomotion. Verification tests were executed with AR601M humanoid robot.

1 INTRODUCTION

Nowadays the interest to humanoid robots rapidly increases. A significant number of successful humanoid solutions and experiments have been demonstrated in the past decades by different research groups and companies, including such as ASIMO (Sakagami et al., 2002), ATLAS (Feng et al., 2015), HRP-4C (Kajita et al., 2010), Wabian (Ogura et al., 2006), AR601M (Khusainov et al., 2015) and others (Shamsuddin et al., 2011) (Ha et al., 2011). However, bipedal robot walking still remains a challenging research topic due to its complexity. One of the most ambitious goals is creating a universal robot that could operate in dynamic environments and replace a human in dangerous operations, e.g., supporting astronauts during space flights or acting in a proximity of a nuclear energy source, chemically or biologically contaminated environments. An obvious advantage of anthropomorphic robots is their ability to apply humanlike skills in order to utilize existing human-oriented technologies and devices. Thus, robust omnidirectional locomotion of a bipedal robot in environments with obstacles becomes crucial to perform such operations effectively.

Robot autonomous performance is another important issue since human teleoperation is not always possible. In order to increase robot capabilities different simultaneous localization and mapping (SLAM) algorithms are used (Stasse et al., 2006). Robot stereo cameras or laser scanners are used to detect surrounding objects and find robot relative position. Such algorithms can generate an optimal and safe trajectory from an initial location to a goal location (Figure1). Next, the robot should generate steps' pattern along the given trajectory based on robot kinematic constraints so that a walking engine could utilize this pattern to perform stable locomotion.

For example in (Strom et al., 2010) authors demonstrated an omnidirectional walking foot planner for NAO robot. In (Zhao et al., 2012) 3D foot planner was demonstrated, which enables robot to maneuver through 3D structures. In (Chestnutt et al., 2005) authors present a footstep planner for the Honda ASIMO robot. However, the effect of kinematic limits in robot leg joints on step parameters has not been studied thoroughly.

In our work we developed an algorithm that generates desired foot positions of the robot for any given trajectory of motion taking into account kinematic limits in robot legs. Then a foot pattern is fed to preview control approach based walking engine, which provides walking along arbitrary trajectory. Additionally, we estimate errors in position and orientation upon reaching the goal location.

The rest of the paper is organized as following. Section 2 describes a foot planner algorithm. Section 3 presents a biped robot walking engine. Section 4 demonstrates experiment results. Finally, Section 5 presents conclusions and future work.

2 FOOT PLANNER

Multiple robot motion planning approaches exist. One of them computes velocity vector and future foot positions based on a current state and desired walking velocity vector (Shafii et al., 2015) (Strom et al., 2010). However, this approach becomes invalid in the presence of obstacles on the robot path, and thus a foot planner algorithm could be applied only after safe path calculation.

An effective foot planner algorithm should be capable to process a trajectory of any complexity with an arbitrary number of obstacles. A desired robot trajectory serves as an input to our algorithm, while foot patterns - positions and orientations of feet for each step along the path - are its output. We present the desired path parametrically with functions $x(t)$ and $y(t)$, defining points on the curve for each $t = 1, 2...N$, where N is the number of points (Figure 1).
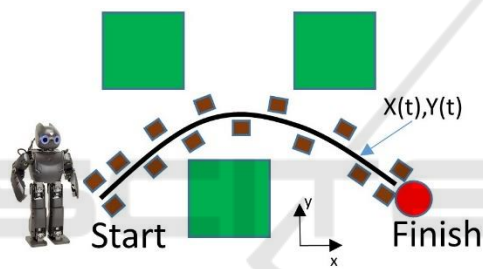

Figure 1: Desired trajectory as an input to foot planner.

Other input parameters for the foot planner are maximum step length L_{max}, maximum rotation angle for a single step θ_{max}, and a distance between foot center and a closest point on the desired path. These values are determined by robot's kinematic constraints. In Figure 2 step length is L, rotation angle is θ and distance between feet is *offset*. Also, it is required to determine stepping order, i.e. which foot makes a first step.

The flowcharts of the proposed foot planner algorithm are presented in Figures 3-4. Here *Planner* is a main function that defines step sequence. It begins with initializing empty arrays for left and right foot coordinates and a center point (x_p, y_p, teta), which is located on a desired curve. Let k be the value of t parameter for point (x_p, y_p). At the beginning of the curve x_p=0, y_p=0, k=1. In other words, a desired path always starts from point (0,0) with zero orientation.

We are moving along the curve by calling *NextPoint* function, which calculates next reachable center point position and orientation. The idea of
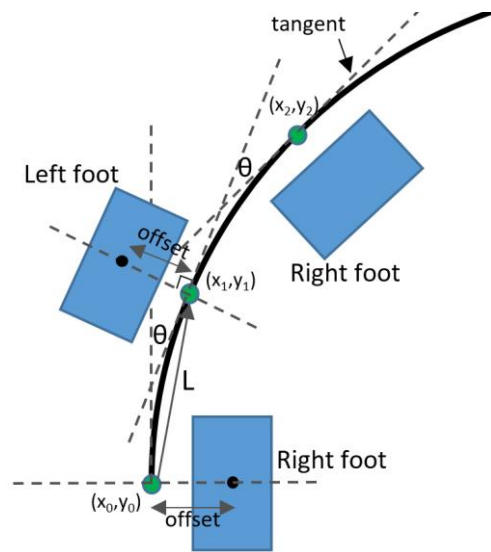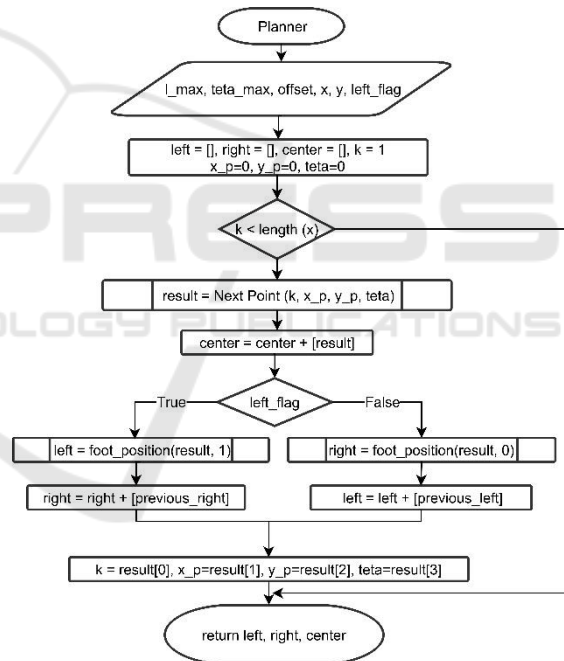

Figure 2: Foot planner parameters.

Figure 3: Foot planner flowchart: *Planner* function (main).

NextPoint function is to decrease step length gradually from L_{max} to 0 by 1 cm until the difference of orientation angles between the current point and previous point becomes lower or equal to θ_{max}. If step length decreases to 0, we make only rotation by angle θ_{max} with no change in position. For the known center point coordinates, *foot_position* function allows us to compute positions of left/right foot center. *Planner* function stops when we get to the last point of the curve.
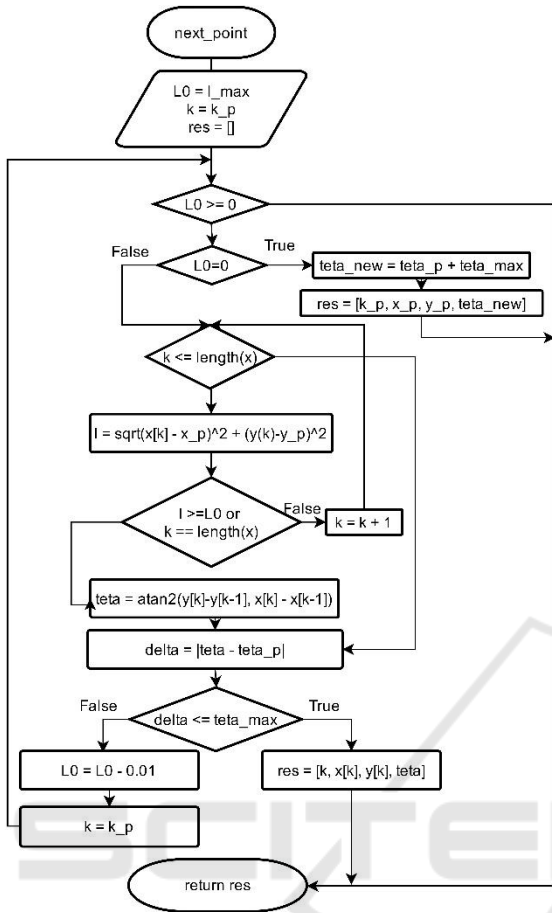
Figure 4: Foot planner flowchart: *next_point* function.

```
function foot_position(left,x,y,teta)
    if left==true
        x=x-offset*cos(teta)
        y=y-offset*sin(teta)
    else
        x=x-offset*cos(teta)
        y=y-offset*sin(teta)
    return (x, y, teta)
end function
```

To illustrate the algorithm, let us consider a sinusoidal curve and run the foot planner for different maximum rotation angle per step θ_{max}. In this case, the desired path is defined as the following:

$$
\begin{aligned}
t &= 1, 2..100 \\
x &= 0.1 - 0.1cos(4\pi(t)/(100)) \\
y &= 0.01t
\end{aligned}
\tag{1}
$$

Simulation results of step planner for $\theta_{max}=5^0$, 10^0 and 15^0 are shown in Figure 6. Here foot positions and orientations are presented as vectors. When maximum rotation angle increases, less steps are required to overcome motion direction change and

complete the path. Table 1 shows number of steps required to complete the considered path for various maximum step lengths and rotation angles. The results highlight stronger dependence of the number of steps (which is proportional to motion time) on the rotation angle than on the step length. The direct correlation between path complexity (convolution and curvature) and stronger dependency on maximum rotation angle is obvious.
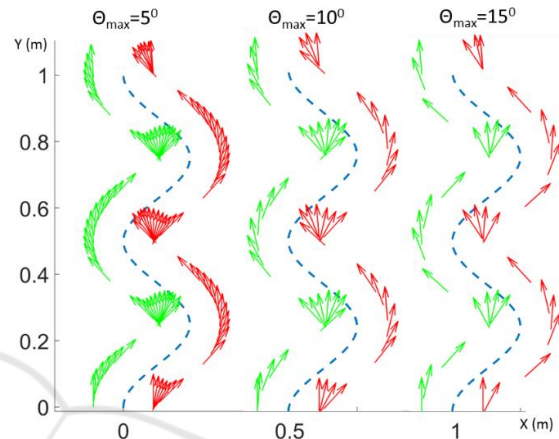

Figure 5: Foot patterns for different maximum rotation angles.

Table 1: Number of steps for different parameters of foot planner so it is centered.

	$L_{max}=10$ cm	$L_{max}=15$ cm	$L_{max}=20$ cm
$\theta_{max}=5°$	109 steps	101 steps	85 steps
$\theta_{max}=10°$	54 steps	54 steps	46 steps
$\theta_{max}=15°$	37 steps	37 steps	33 steps

We emphasize that the foot planner is a part of robot locomotion control. It defines foot positions but does not determine robot motion between the consequent steps and does not consider walking stability. The latter problem is in the focus of the walking engine, which we describe in the next section. Also, it should be noted that the process of trajectory generation is not in the focus of this work. The algorithm considered in the paper deals with pre-defined trajectory.

3 WALKING ENGINE

To achieve walking functional, we decompose the engine into several modules and consider each module independently. Figure 7 shows all modules and interaction between them; description of each module is given below.
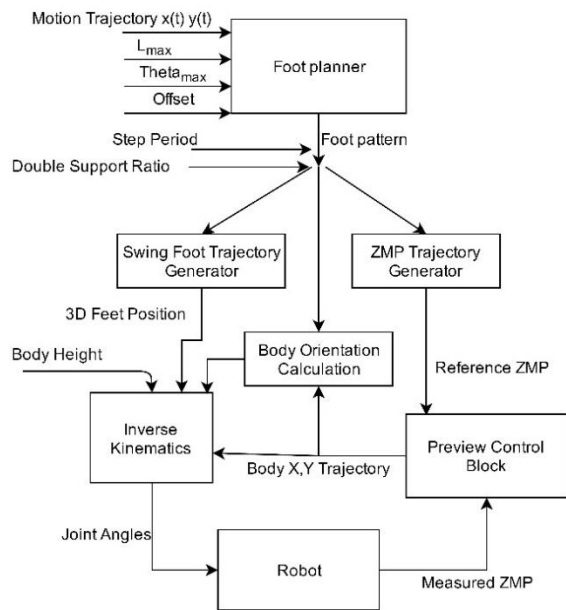
Figure 6: Architecture of walking engine.

3.1 Foot Planner

Foot planner workflow was described in previous section. We initialize it with a desired path and step parameters and it returns a set of feet center positions and orientations along the desired path.

3.2 Swing Foot Trajectory Generator

To generate swing foot trajectory, we need coordinates and orientation at the beginning and at the end of the step, which are provided by the foot planner. The aim of a swing foot trajectory generator is to obtain time dependant functions for the Cartesian coordinates x, y, z, θ, where θ corresponds to the foot rotation around z axis. There are many ways to do it. For example in (Rai and Tewari) authors use a polynomial interpolation to obtain a swing leg trajectory. In (Khusainov et al., 2016) optimal swing leg trajectory is obtained, taking into account joint kinematic limits. Here we used trigonometric functions to build trajectory profile, since they are simple and can provide zero velocities at contact moments. Assuming that x_s and x_f are coordinates at start and end of a step calculated by the foot planner, t_{ds} is double support phase time, t_{ver} is vertical motion time, t_0 is step time, x(t) can be written as:

$$x = x_s, \ if \ t \le t_{ds}$$

$$x = 0.5\left(x_f - x_s\right)\left(1 - cos\left(\frac{\pi\left(t - t_{ds}\right)}{\left(t_0 - t_{ds} - t_{ver}\right)}\right)\right) + x_s, \quad (1)$$

$$if \ t_{ds} < t \le t_0 - t_{ver}$$

$$x = x_f, \ if \ t > t_0 - t_{ver}$$

At the end of the step there is an interval t_{ver} with no motion in x-direction. We introduced this to ensure strictly vertical motion of the swing foot before touching the surface and to avoid horizontal momentum at a contact. Also, it should be noted that cosine function gives zero velocity values at the beginning and at the end of motion. Equations for y(t) and θ(t) are similar, while z(t) coordinate function is presented as:

$$z = 0, \ if \ t \le t_{ds}$$

$$z = 0.5h\left(1 - cos\left(2\pi\left(t - t_{ds}\right)/\left(t_0 - t_{ds}\right)\right)\right), \quad (2)$$

$$if \ t > t_{ds}$$

where h is a step height. In this work we assume that the swing foot is always parallel to the ground.

3.3 ZMP Trajectory Generator

A zero-moment point (ZMP) criterion is widely used as a stability measure in the literature (Vukobratović and Borovac, 2004) (Lee et al., 2015). To ensure stable locomotion of the robot, a ZMP point should lie within supporting polygon, which is the convex hull of supporting feet area (Vukobratović and Stepanenko, 1972). Therefore, we can introduce some reference ZMP trajectory, which always lies within supporting polygon and compute feasible robot center of mass (CoM) trajectory so that its ZMP follows the reference ZMP. Reference ZMP functions for x and y coordinates, which are the input values for the controller, are computed from supporting foot center coordinates, which in turn is calculated from foot positions and step time. Suppose that robot starts walking straight ahead with a distance of 20 cm between the feet. In Figure 8 the reference ZMP is initially located in the center of right foot (supporting foot) with coordinate -10 cm, then moves to the center of left foot with coordinate +10 cm and so on. Duration of ZMP change is defined by double support phase time during which both legs are on the ground. To obtain smooth change of ZMP value we used cubic spline in a double support phase.
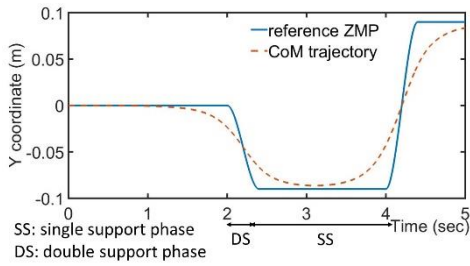
Figure 7: Reference ZMP and CoM trajectory in sagittal plane.

3.4 Preview Control Block

Preview control block generates CoM trajectory based on the reference ZMP and active balance feedback loop. The CoM trajectory can be calculated by a simple physical model approximating the bipedal robot dynamics. In our work we use preview control approach (Kajita et al., 2003) and describe robot dynamics by inverted pendulum model with additional constraint on mass height, i.e., three-dimensional linear inverted pendulum model. There are several assumptions in this model.
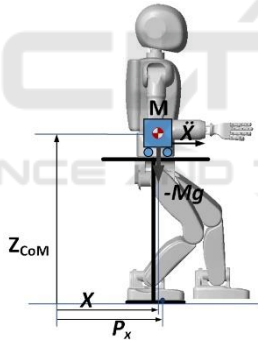

Figure 8: Cart-table model for bipedal locomotion.

The first assumption is that all mass is concentrated in CoM point, which means that we neglect mass distribution and suppose that leg's mass is relatively small. Although this assumption seems to differ from reality, effect of leg's mass can be neglected at a first approximation, since robot's trunk is much heavier than a leg. The second assumption is that CoM always keeps a constant height. This assumption significantly simplifies dynamics equations. A cart-table model, shown in Figure 9, corresponds to the described model. The cart with mass M moves on a table with a negligible mass. ZMP coordinate in this case can be written as:

$$p_x = x - \frac{z_{CoM}}{g}\ddot{x} \qquad (3)$$

where x and $\ddot{x}$ are CoM coordinate and acceleration, g is gravity constant, z_{CoM} is CoM height. For 3D walking we use two cart-table models, one is for motion in a sagittal plane, the other is for motion in a frontal plane. Therefore, y coordinate equation could be written similarly to (4):

$$p_y = y - \frac{z_{CoM}}{g}\ddot{y} \qquad (4)$$

If CoM trajectory is given, we can easily calculate ZMP by using ZMP equations (4) and (5). On the other hand, for stable motion ZMP should always lie under a supporting foot. Therefore, we can determine reference ZMP trajectory knowing supporting foot coordinates as a function of time. Hence, we have an inverse problem, where CoM trajectory is calculated from reference ZMP trajectory.

If we define new variable as $u = \dddot{x}$, equation (4) can be rewritten as dynamical system equation:

$$\frac{d}{dt}\begin{bmatrix} x \\ \dot{x} \\ \ddot{x} \end{bmatrix} = \begin{bmatrix} 0 & 1 & 0 \\ 0 & 0 & 1 \\ 0 & 0 & 0 \end{bmatrix}\begin{bmatrix} x \\ \dot{x} \\ \ddot{x} \end{bmatrix} + \begin{bmatrix} 0 \\ 0 \\ 1 \end{bmatrix}u$$

$$p_x = \begin{bmatrix} 1 & 0 & z_{CoM}/g \end{bmatrix}\begin{bmatrix} x \\ \dot{x} \\ \ddot{x} \end{bmatrix} \qquad (5)$$

Then the system can be discretized as

$$x(k+1) = Ax(k) + Bu(k)$$
$$p(k) = Cx(k) \qquad (6)$$

where A, B and C matrices are found from (6), k is a discrete time, x is a state vector, u is a jerk and p is a ZMP coordinate. (Katayama et al., 1985) presented a preview control approach that uses a desired future value of the ZMP coordinates. Authors showed that the optimal controller for the system with given reference ZMP p_{ref} and previewing N future steps can be written as:

$$u(k) = -G_i \sum_{i=0}^{k} e(k) - G_x x(k) - \sum_{j=1}^{N} G_p(j)p_{ref}(k+j) \quad (7)$$

where G_i, G_x and $G_p(j)$ are gains that are calculated from controller weights, $e(k) = p(k) - p_{ref}(k)$ is a ZMP error. Thus, the preview controller consists of three terms: the integral error of ZMP, the state feedback (that is proportional to a current state vector

x) and the preview action, which takes into account future values of the desired ZMP position with the sum running over N future values. Figure 8 shows reference ZMP and calculated CoM trajectory in the frontal plane. Here CoM starts moving before a sharp change of reference ZMP, which is an effect of previewing the future reference.

3.5 Body Orientation

Preview controller computes x_{CoM} and y_{CoM} of the body with z_{CoM} being fixed. There remains 3 DoF for body orientation definition and 6 DoF undetermined for swing foot. We put some additional constraints on the system by setting to zero trunk Y axis rotation, which means there is no forward-backward inclination of the trunk. Trunk X axis rotation is defined by its side inclination. This is done because of kinematic limits in hip and ankle roll joints. Suppose that robot stands with parallel feet on the ground. If we start moving trunk to its right and remain it upright, at some point we will hit kinematic limits (marked red in Figure 10).
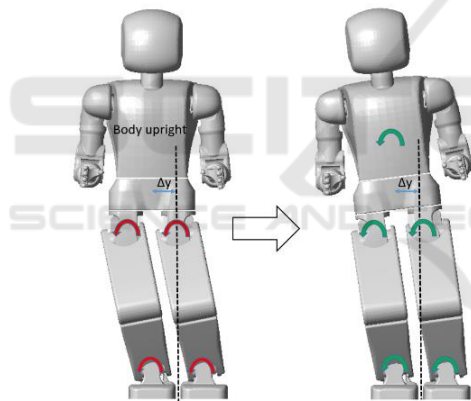

Figure 9: Body orientation in frontal plane.

Therefore, we should rotate trunk around X axis. To find the rotation angle we first calculated all possible trunk rotation angles for a given joint limits and trunk y coordinate by applying inverse kinematic problem (see section 3.5). Then we took the middle value of interval as the best rotation angle. Figure 11 shows trunk X axis rotation angle as a function of trunk y coordinate. z_{CoM} was set to 0.7 m, maximum hip roll rotation angles were 0.2 rad for inward and 0.3 rad for outward rotation. We see piecewise linear uneven function which can be approximated as:

$$\theta = -1.67\,y,\ if\ y \le 0.0228$$
$$\theta = -0.8295\big(y - 0.0228\big) - 0.038076, \qquad (8)$$
$$if\ y > 0.0228$$

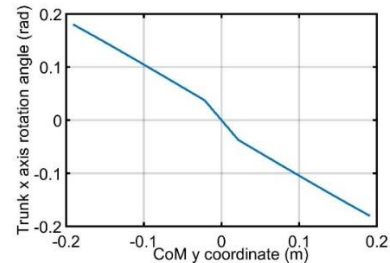Function (9) gives us optimal trunk rotation angle for given CoM y coordinate.

Figure 10: Dependency of optimal rotation angle on CoM y coordinate.

3.6 Inverse Kinematics

After we have fully defined all 6 DoF for each leg the next step is to solve inverse kinematics problem for each leg, i.e. to find joint angles given the position and orientation of foot and torso.
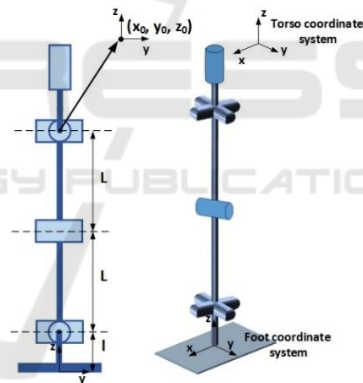

Figure 11: Leg kinematic scheme.

(Peiper, 1968) showed that if three adjacent joint axes intersect in a single point, there exists closed-form solution of the inverse kinematics problem. In our scheme (Figure 12) we have this condition for hip joints. Given transformation matrix from global coordinate system (CS) to torso CS is T_t and from global CS to foot CS is T_f, then we can write transformation matrix from foot to torso system is $T_{ft} = T_t T_f^{-1}$. At the same time

$$T_{ft} = T_1(\theta_1)T_2(\theta_2)T_3(\theta_3)T_4(\theta_4)T_5(\theta_5)T_6(\theta_6) \qquad (9)$$

where $\theta_1...\theta_6$ are joint angles, starting from ankle roll angle. Since last three rotations do not effect on hip

joints center position, we firstly find $\theta_1, \theta_2, \theta_3$ angles. After that we substitute calculated angles into (10) and compare rotation matrices of T_{ft} matrix and product matrix to find remaining three angles. There are totally eight possible solutions of inverse kinematics problem so we choose appropriate one.

4 EXPERIMENTAL RESULTS

To demonstrate the proposed algorithm efficiency we verified its performance with AR-601M bipedal robot (Figure 13). The robot has totally 41 active degrees of freedom (DoF), 6 of which are located in each leg: three joint axes are in the hip, two joints are at the ankle and one in the knee. The total mass of the robot is 65 kg and the height is 1442 mm. Further details about AR-601M are available in (Khusainov et al., 2015).

Figure 12: Humanoid robot AR601M.

Two trajectories were tested in experimental study. The first experiment was walking for 2 m distance along a straight line. The robot's step length was set to 15 cm with the step period of 3 seconds. Figure 14 shows foot pattern, CoM trajectory and ZMP trajectory measured with force sensors. The second trajectory was defined as sinusoid curve. Step length was set to 15 cm, maximum rotation angle to 10^0, and the step period to 3 seconds and the experimental data is presented in Figure 15.

Results for average coordinate errors with respect to the desired goal position are given in Table 2. These differences were mainly caused by compliance in actuator joints and errors (and noise) of the sensors. Yet, these errors are acceptable for the considered distances and do not overcome 3%. For larger distances, these errors should be compensated by external position control, e.g., SLAM methods.
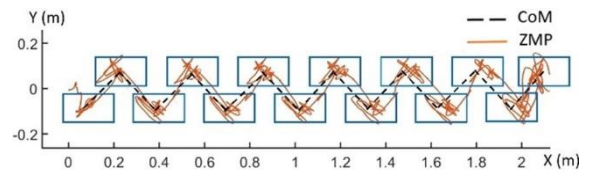

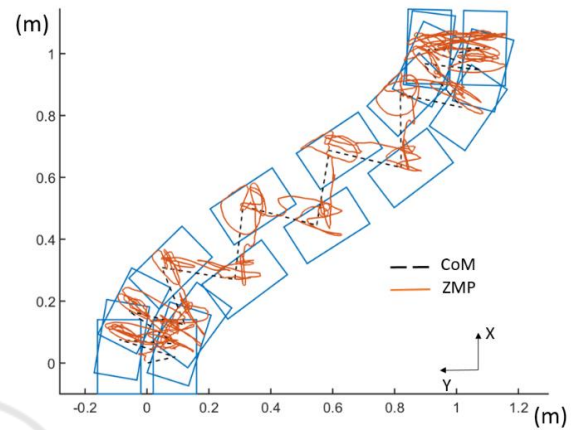Figure 13: Experimental results: walking on a straight line.

Figure 14: Experimental results: walking along a curve.

Table 2: Average error for position and orientation.

	Δx cm	Δy cm	$\Delta\theta$ deg
Straight line	1.5	5	5°
Along a curve	3	3	5°

5 CONCLUSIONS

This paper presents the foot planner algorithm for biped walking along an arbitrary curve. Together with the walking engine, it enables the robot to move along a desired path with acceptable position and orientation errors. Preview control method was used as a walking engine balance controller.

The presented biped locomotion approach was verified with a AR601M robot. Experimental results illustrated successful performance of the proposed foot planner method and walking engine architecture. However, because of accumulated errors of different nature, for large walking distances our algorithm would require additional external system to measure position error, which could provide a feedback loop and significantly increase position accuracy.

ACKNOWLEDGEMENTS

REFERENCES

Chestnutt, J., Lau, M., Cheung, G., Kuffner, J., Hodgins, J. and Kanade, T. 'Footstep Planning for the Honda ASIMO Humanoid'. *Proceedings of the 2005 IEEE International Conference on Robotics and Automation*, 18-22 April 2005, 629-634.

Feng, S., Whitman, E., Xinjilefu, X. and Atkeson, C. G. (2015) 'Optimization- based Full Body Control for the DARPA Robotics Challenge', *Journal of Field Robotics,* 32(2), pp. 293-312.

Ha, I., Tamura, Y., Asama, H., Han, J. and Hong, D. W. 'Development of open humanoid platform DARwIn-OP'. 2011: IEEE, 2178-2181.

Kajita, S., Kanehiro, F., Kaneko, K., Fujiwara, K., Harada, K., Yokoi, K. and Hirukawa, H. (2003) 'Biped walking pattern generation by using preview control of zero-moment point'. *Robotics and Automation, 2003. Proceedings. ICRA '03. IEEE International Conference on*, 14-19 Sept. 2003, 1620-1626 vol.2.

Kajita, S., Morisawa, M., Miura, K., Nakaoka, S. i., Harada, K., Kaneko, K., Kanehiro, F. and Yokoi, K. 'Biped walking stabilization based on linear inverted pendulum tracking'. 2010: IEEE, 4489-4496.

Katayama, T., Ohki, T., Inoue, T. and Kato, T. (1985) 'Design of an optimal controller for a discrete-time system subject to previewable demand', *International Journal of Control,* 41(3), pp. 677-699.

Khusainov, R., Klimchik, A. and Magid, E. 'Swing leg trajectory optimization for a humanoid robot locomotion'. *Informatics in Control, Automation and Robotics (ICINCO), 2016 13th International Conference on*.

Khusainov, R., Shimchik, I., Afanasyev, I. and Magid, E. 'Toward a human-like locomotion: Modelling dynamically stable locomotion of an anthropomorphic robot in simulink environment'. *Informatics in Control, Automation and Robotics (ICINCO), 2015 12th International Conference on*, 21-23 July 2015, 141-148.

Lee, D.-W., Lee, M.-J. and Kim, M.-S. 'Whole body imitation of human motion with humanoid robot via ZMP stability criterion'. 2015: IEEE, 1003-1006.

Ogura, Y., Aikawa, H., Shimomura, K., Kondo, H., Morishima, A., Lim, H.-o. and Takanishi, A. (2006) 'Development of a new humanoid robot WABIAN-2'. 2006: IEEE, 76-81.

Peiper, D. L. (1968) *The kinematics of manipulators under computer control*: DTIC Document.

Rai, J. K. and Tewari, R. 'Quintic polynomial trajectory of biped robot for human-like walking'. 2014: IEEE, 360-363.

Sakagami, Y., Watanabe, R., Aoyama, C., Matsunaga, S., Higaki, N. and Fujimura, K. 'The intelligent ASIMO: System overview and integration'. 2002: IEEE, 2478-2483.

Shafii, N., Abdolmaleki, A., Lau, N. and Reis, L. P. (2015) 'Development of an Omnidirectional Walk Engine for Soccer Humanoid Robots'.

Shamsuddin, S., Ismail, L. I., Yussof, H., Zahari, N. I., Bahari, S., Hashim, H. and Jaffar, A. 'Humanoid robot NAO: Review of control and motion exploration'. 2011: IEEE, 511-516.

Stasse, O., Davison, A. J., Sellaouti, R. and Yokoi, K. 'Real-time 3D SLAM for Humanoid Robot considering Pattern Generator Information'. *2006 IEEE/RSJ International Conference on Intelligent Robots and Systems*, Oct. 2006, 348-355.

Strom, J., Slavov, G. and Chown, E. (2010) 'Omnidirectional Walking Using ZMP and Preview Control for the NAO Humanoid Robot', in Baltes, J., Lagoudakis, M., Naruse, T. & Ghidary, S. (eds.) *RoboCup 2009: Robot Soccer World Cup XIII Lecture Notes in Computer Science*: Springer Berlin Heidelberg, pp. 378-389.

Vukobratović, M. and Borovac, B. (2004) 'Zero-moment point — thirty five years of its life', *International Journal of Humanoid Robotics,* 01(01), pp. 157-173.

Vukobratović, M. and Stepanenko, J. (1972) 'On the stability of anthropomorphic systems', *Mathematical biosciences,* 15(1-2), pp. 1-37.

Zhao, Y. and Sentis, L. 'A three dimensional foot placement planner for locomotion in very rough terrains'. *2012 12th IEEE-RAS International Conference on Humanoid Robots (Humanoids 2012)*, Nov. 29 2012-Dec. 1 2012, 726-733.